

# Millimeter-Wave Vector Signal Generation Based on a Bi-Directional Use of a Polarization Modulator in a Sagnac Loop

Ruoming Li, *Student Member, IEEE*, Wangzhe Li, *Student Member, IEEE*, Xiangfei Chen, *Senior Member, IEEE*, and Jianping Yao, *Fellow, IEEE, Fellow, OSA*

**Abstract**—A novel technique to generate a frequency-doubled millimeter-wave (mm-W) vector signal that is immune to fiber chromatic-dispersion-induced power fading and free from inter-band beating interferences (IBBIs) based on a bi-directional use of a polarization modulator (PolM) in a Sagnac loop is proposed and experimentally demonstrated. The fundamental concept of the proposed approach is to use a PolM that is incorporated in a Sagnac loop at which a light wave is modulated by an intermediate-frequency vector signal along one direction and with no modulation along the opposite direction due to the traveling-wave nature of the PolM. The combination of the modulated and un-modulated signals at a photodetector will generate an mm-W signal that is immune to the fiber chromatic-dispersion-induced power fading and free from the IBBIs. The generation of a 100 and a 500 MSym/s 16-QAM signal at 31.5 GHz and the transmission of the signals over a 25-km single-mode fiber are evaluated. An error-free transmission of the 100 MSym/s signal and the transmission of the 500 MSym/s signal with a bit-error-rate below the forward error correction threshold of  $3.8 \times 10^{-3}$  are achieved.

**Index Terms**—Microwave photonics, optical millimeter-wave generation, polarization modulation, radio-over-fiber systems, vector signal generation.

## I. INTRODUCTION

As a potential solution to provide services for broadband wireless access, the distribution of radio signals over optical fibers, known as radio over fiber (RoF), has been intensively investigated for the last few years. Owing to the continuously growing data rate, wireless access networks operating at the millimeter-wave (mm-W) band are considered a solution to fulfil the bandwidth demand. However, for an access network operating in the mm-W band, the system cost would increase significantly due to the very high frequency. A solution is to use relatively low-frequency opto-electronic components to

generate high-frequency mm-W signals [1]. In addition, the use of advanced modulation schemes can significantly improve the spectral efficiency and thus further reducing the overall system cost [2].

One simple way to generate an mm-W signal using low-frequency components is to use the widely known optical carrier-suppressed (OCS) modulation scheme [3]–[5]. Since the optical carrier is suppressed, the beating between the two first-order sidebands will generate a frequency-doubled signal, thus the OCS modulation scheme is more cost-effective than the optical double-sideband (DSB) modulation scheme [6] and the optical single-sideband modulation (SSB) scheme [7]. The major limitation of the OCS modulation scheme is that it is unable to carry a vector signal directly [3] [8]–[10]. A few schemes have been proposed to generate an mm-W vector signal, such as the use of digital pre-distortion coding to encode a vector signal before employing the OCS modulation scheme [3] or the frequency-quadrupling modulation scheme [8]. However, the pre-distortion coding is signal modulation format dependent. For multi-format signal transmission, a dedicated pre-coding method for each signal is needed, which will complicate the system implementation. The use of the heterodyne OCS modulation scheme [9], which is based on the OCS-modulation structure with an optical filter employed to selectively remove the redundant sidebands, can also generate a vector-signal-modulated mm-W signal without the need of pre-distortion coding. The major limitation of the heterodyne OCS modulation scheme is that an optical filter with a well-tailored spectral response is needed to select the required optical carriers and sidebands, which would increase the system complexity and cost. Furthermore, the transmission of an optical signal generated based on the heterodyne OCS modulation scheme may suffer from the chromatic-dispersion-induced power-fading effect. Another approach to generating a vector signal without using a complicated optical filter was proposed in [10]. In the scheme, two optical carriers generated by biasing a Mach-Zehnder modulator (MZM) at the minimum transmission point are sent to an optical interleaver to physically separate the two optical carriers. One optical carrier is phase modulated and recombined with the unmodulated optical carrier, and then both carriers are sent to a second MZM to perform amplitude modulation. A vector signal is thus generated at the output of the second MZM. The major limitation of the approach is that the two optical carriers are physically separated and recombined, which would cause phase fluctuations due to environmental disturbance. In

Manuscript received August 4, 2014; revised October 20, 2014 and December 1, 2014; accepted December 1, 2014. Date of publication December 7, 2014; date of current version January 23, 2015. This work was supported by the Natural Sciences and Engineering Research Council of Canada. The work of R. Li was supported by a scholarship from the China Scholarship Council.

R. Li is with the Microwave Photonics Research Laboratory, School of Electrical Engineering and Computer Science, University of Ottawa, Ottawa ON K1N 6N5, Canada, and also with the College of Engineering and Applied Sciences, Nanjing University, Nanjing 210093, China.

W. Li and J. Yao are with the Microwave Photonics Research Laboratory, School of Electrical Engineering and Computer Science, University of Ottawa, Ottawa, ON K1N 6N5, Canada (e-mail: jpyao@eecs.uOttawa.ca).

X. Chen is with the College of Engineering and Applied Sciences, Nanjing University, Nanjing 210093, China.

Color versions of one or more of the figures in this paper are available online at <http://ieeexplore.ieee.org>.

Digital Object Identifier 10.1109/JLT.2014.2379473

addition, the approach does not support the generation of some widely used vector signals of which the amplitudes of the in-phase and quadrature-phase components are equal such as the square quadrature amplitude modulation (QAM) signal.

Microwave vector signals can also be generated based on I/Q modulation. In [11], two baseband I/Q signals are combined separately with two microwave signals with an identical frequency but a  $90^\circ$  phase difference. The two combined signals are applied to a dual-parallel MZM with direct detection or two MZMs with balanced detection [12], to generate an optical microwave vector signal. Microwave vector signals can also be generated by introducing a  $90^\circ$  phase shift to the envelope of an optical field using a delay line [13] or a dispersive device [14]. However, for the schemes in [11]–[14], the microwave frequency is again limited by the bandwidth of the electro-optic modulators.

In addition, for an intensity-modulation direct-detect RoF system supporting multiple RF band operation, the use of the OCS scheme in [3]–[5], [8], [10] will cause inter-band beating interferences (IBBIs), and thus deteriorating the overall system performance.

In this paper, we propose a novel approach to generating a frequency-doubled mm-W vector signal that is immune to the fiber chromatic-dispersion-induced power fading and free from the IBBIs based on a bi-directional use of a polarization modulator (PolM) in a Sagnac loop. In the proposed system, two orthogonally polarized optical sidebands, which are generated by an MZM biased at the minimum transmission point and a polarization-maintaining fiber Bragg grating (PM-FBG) are sent to the Sagnac loop via a polarization beam splitter (PBS). A 16-QAM signal at an intermediate frequency (IF) is applied to the PolM that is incorporated in the Sagnac loop. The PolM is a traveling-wave device, which modulates the light wave in a uni-directional manner in the loop, leaving light wave in the other direction unmodulated due to the velocity mismatch [15]. Since the two carriers are separated and only one carrier is DSB modulated by the IF signal, the power fading effect is completely eliminated. In addition, the components due to the inter-band beating are located out of the mm-W band, thus the proposed system is free from IBBIs. Furthermore, the ratio between the powers of the unmodulated optical carrier and the signal sideband can be easily tuned, and as a result, the scheme provides a way to optimize the performance of the generated signal by controlling the power ratio.

An experiment is performed to evaluate the performance of the proposed system. The generation of a 100 and a 500 MSym/s 16-QAM signal at 31.5 GHz and the transmission of the signals over a 25-km single mode fiber (SMF) are evaluated. An error-free transmission of the 100 MSym/s signal and the transmission of the 500 MSym/s signal with a bit-error-rate (BER) below the forward-error correction (FEC) threshold of  $3.8 \times 10^{-3}$  are achieved.

## II. PRINCIPLE

Fig. 1 shows the schematic of the proposed mm-W vector signal generation system and the transmission of the signals over a WDM-PON. In a transmitter, an mm-W vector signal is

generated based on a bi-directional use of a PolM in a Sagnac loop. At the optical line terminal (OLT), the wavelengths from the transmitters are multiplexed at a multiplexer (MUX) and sent to a remote access node (RAN) through a shared optical link after amplification by an erbium-doped fiber amplifier (EDFA). The WDM channels are then demultiplexed by a demultiplexer (DE-MUX) at the RAN, and each wavelength is sent to the corresponding optical network unit (ONU).

Specifically, in a transmitter a light wave from a laser diode (LD) is sent through a polarization controller (PC1) to an MZM. The MZM is biased at the minimum transmission point to suppress the optical carrier and generate two first-order sidebands, serving as two new optical carriers. To increase the power of the two first-order sidebands for improving the transmission performance of the system [16], a large RF drive signal is applied to the MZM. A programmable optical filter (POF, Finisar Wave-Shaper 4000S) is connected after the MZM to select only the two first-order sidebands, and eliminate the residual optical carrier and the higher order sidebands. The two sidebands are sent to a PM-FBG through a second PC (PC2). Owing to the birefringence in the polarization-maintaining fiber, the PM-FBG has two orthogonally polarized and spectrally separated transmission bands [17]. By passing the two sidebands through the two transmission bands, the two sidebands become orthogonally polarized, which are then launched into a Sagnac loop via a third PC (PC3) and a PBS. The Sagnac loop consists of a PolM and two PCs (PC4 and PC5), as shown in Fig. 1. The two orthogonally polarized sidebands are fed into the Sagnac loop via the PBS, with one sideband sent to the PolM along the clockwise direction and the other to the PolM along the counter-clockwise direction. Note that the PolM is a traveling-wave device; for a light wave traveling along the counter-clockwise direction, the velocities of the light wave and the modulating signal are matched, and thus the light wave is effectively modulated. Due to the velocity mismatch, the light wave traveling along the clockwise direction is very weakly modulated [18]. Note also that the PolM is a special phase modulator that supports phase modulation along the two principal axes with opposite modulation indices. The joint operation of the PolM, PC5, and the PBS corresponds to an MZM with the bias point determined by the static phase which is introduced by applying a bias voltage to the PolM or simply by using PC5 [19]. A 16-QAM IF signal generated by an arbitrary waveform generator (AWG) is then applied to the PolM. Due to the velocity mismatch, the 16-QAM IF signal is not modulated on the clockwise light wave, but it is effectively modulated on the counter-clockwise light wave. In the analysis, we take the two orthogonal directions (the two principal axes) of the PM-FBG as the reference directions of the system. The principle axes of the PBS and the PolM are aligned to the reference directions. Both PC4 and PC5 introduce a  $45^\circ$  rotation of the polarization to the bi-directionally transmitted light waves. At the output of the Sagnac loop, the two light waves are recombined at the PBS, and multiplexed with other channels at the MUX. After being amplified by the EDFA, the signals from all transmitters are sent to the RAN over the SMF. After being demultiplexed at the DE-MUX, the signals from different transmitters are separated and sent to the corresponding ONUs. At an ONU, the two orthogonally polarized light waves

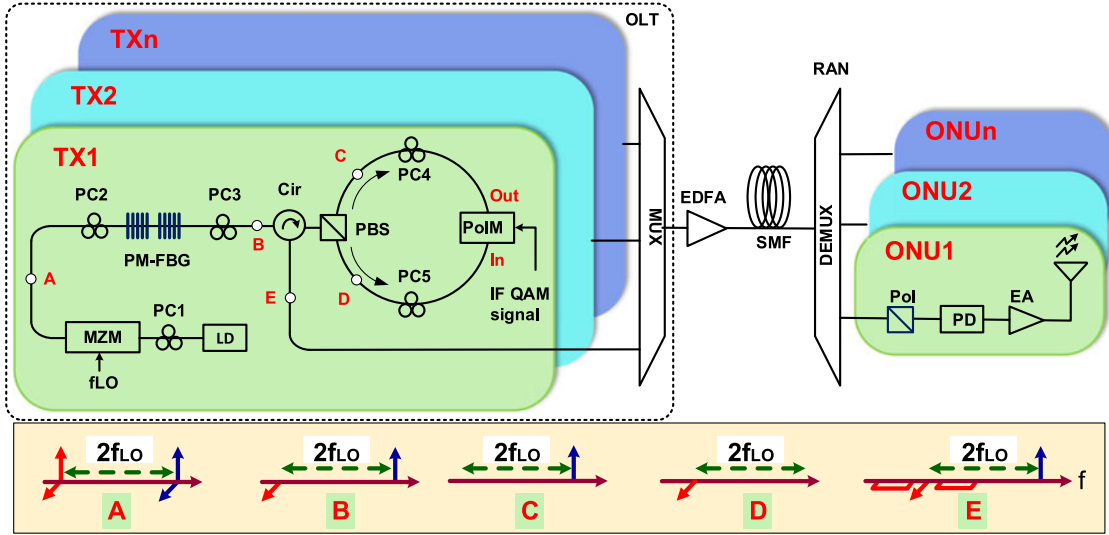


Fig. 1. Bi-directional polarization modulation technique based WDM-PON architecture LD, laser diode; OLT, optical line terminal; MUX, WDM multiplexer; RAN, remote access node; DEMUX, WDM demultiplexer; ONU, optical network unit; PBS, polarization beam splitter; Pol, polarizer; PM-FBG, polarization maintaining fiber Bragg gratings; Cir, circulator; EA, electronic amplifier; PC, polarization controller; EDFA, erbium-doped fiber amplifier; TX, transmitter.

are projected to a polarizer (Pol), of which the principal axis is oriented at an angle of  $45^\circ$  relative to one reference direction, and then applied to a photodetector PD. In the Sagnac loop, since the two light waves are traveling in the same optical path, the relative phase changes between the two optical waves due to environmental disturbances are small, thus ensuring a stable operation.

Mathematically, the IF vector signal can be expressed as

$$S_{\text{IF}}(t) = \sum_{n=0}^{\infty} A_n(t) \sin[\omega_{\text{IF}}t + \theta_n(t)] \text{Rect}(t - nT) \quad (1)$$

where  $A_n(t)$  and  $\theta_n(t)$  are the  $n$ th symbol's amplitude and phase variation of the input signal,  $\omega_{\text{IF}}$  is the angular frequency of the IF carrier, and  $\text{Rect}(t)$  is a rectangular window with a temporal width of  $T$ , given by

$$\text{Rect}(t) = \begin{cases} 0, & t < 0, \quad t > T \\ 1, & 0 < t < T \end{cases}. \quad (2)$$

The electric field of the optical signal at the output of the Sagnac loop can be expressed as

$$\begin{aligned} E_{\text{out}}(t) = & E_0 J_1(\beta_{\text{MZM}} A_{\text{LO}}) \sin[(\omega_0 + \omega_{\text{LO}})t] \\ & + \frac{1}{2} E_0 J_1(\beta_{\text{MZM}} A_{\text{LO}}) \sin[(\omega_0 - \omega_{\text{LO}})t] \\ & \times \{ \cos[\beta_{\text{PoIM}} S_{\text{IF}}(t) + \phi] + \cos[-\beta_{\text{PoIM}} S_{\text{IF}}(t)] \} \end{aligned} \quad (3)$$

where  $\phi$  is the static phase difference between the two orthogonally polarized light waves travelling along the principal axes of the PolM, and it can be adjusted by either tuning the bias voltage applied to the PolM, or simply tuning PC4 or PC5. When  $\phi = \pi/2$ , Eq. (3) can be

simplified to

$$\begin{aligned} E_{\text{out}}(t) = & E_0 J_1(\beta_{\text{MZM}} A_{\text{LO}}) \sin[(\omega_0 + \omega_{\text{LO}})t] \\ & + \frac{1}{2} E_0 J_1(\beta_{\text{MZM}} A_{\text{LO}}) \sin[(\omega_0 - \omega_{\text{LO}})t] \\ & \times \sum_{n=0}^{\infty} \left\{ \begin{aligned} & J_0[\beta_{\text{PoIM}} A_n(t)] \\ & - 2J_1[\beta_{\text{PoIM}} A_n(t)] \sin[\omega_{\text{IF}}t + \theta_n(t)] \end{aligned} \right\} \\ & \times \text{Rect}(t - nT) \end{aligned} \quad (4)$$

where  $E_0$  is the electrical amplitude of the incident light wave, and  $\omega_{\text{LO}}$ , and  $\omega_0$  are the angular frequencies of the LO carrier and the light wave, respectively.  $\beta_{\text{PoIM}}$  and  $\beta_{\text{MZM}}$  are equal to  $\pi/(2V_{\pi\text{PoIM}})$  and  $\pi/(2V_{\pi\text{MZM}})$ , where the  $V_{\pi\text{PoIM}}$  and  $V_{\pi\text{MZM}}$  are the half-wave voltages of the PolM and MZM, respectively.  $J_0$  and  $J_1$  is the Bessel functions of the first kind of orders 0 and 1, and  $A_{\text{LO}}$  is the amplitude of the LO carrier.

The in-band photo-current generated at the PD is given by

$$\begin{aligned} i_{\text{out}}^{\text{RF}}(t) \propto & \frac{1}{2} E_0^2 J_1^2(\beta_{\text{MZM}} A_{\text{LO}}) \\ & \times \sum_{n=0}^{\infty} \left\{ \begin{aligned} & J_0[\beta_{\text{PoIM}} A_n(t)] \cos(2\omega_{\text{LO}}t) \\ & + \{-J_1[\beta_{\text{PoIM}} A_n(t)] \sin[(2\omega_{\text{LO}} + \omega_{\text{IF}})t + \theta_n(t)]\} \\ & + \{J_1[\beta_{\text{PoIM}} A_n(t)] \sin[(2\omega_{\text{LO}} - \omega_{\text{IF}})t - \theta_n(t)]\} \end{aligned} \right\} \\ & \times \text{Rect}(t - nT). \end{aligned} \quad (5)$$

As can be seen from (5) that the input symbol with an amplitude of  $A_n(t)$ , a phase of  $\theta_n(t)$  and a carrier angular frequency of  $\omega_{\text{IF}}$  is converted to a symbol with an amplitude of  $E_0^2 \times J_1^2(\beta_{\text{MZM}} A_{\text{LO}}) \times J_1[\beta_{\text{PoIM}} A_n(t)]$ , a phase of  $\theta_n(t)$ , and a carrier angular frequency of  $2\omega_{\text{LO}} \pm \omega_{\text{IF}}$ .

It is well-known that the transmission of a DSB-modulated mm-W signal over an optical fiber suffers from the chromatic-dispersion-induced power fading. For the proposed scheme,

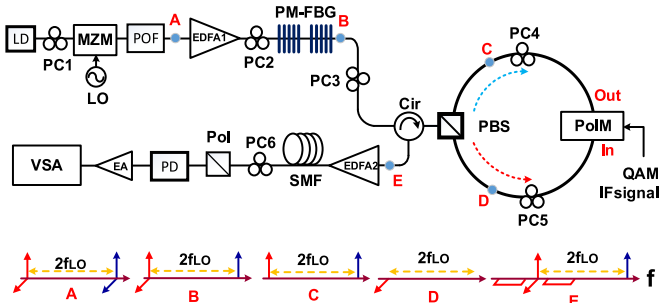


Fig. 2. The experimental setup for the generation of an mm-W 16-QAM signal. LD, laser diode; EDFA, erbium-doped fiber amplifier; MZM, Mach-Zehnder modulator; POF, programmable optical filter; PBS, polarization beam splitter; PolM, polarization modulator; Pol, polarizer; PM-FBG, polarization-maintaining fiber Bragg grating; PD, photodetector; SMF, single-mode fiber; Cir, circulator; EA, electronic amplifier; PC, polarization controller.

assuming that the interested mm-W signal is at  $2\omega_{LO} - \omega_{IF}$ , from (4) and (5) we can see, the mm-W signal is exclusively generated by the beating between the optical carrier at  $\omega_0 - \omega_{LO}$  and the sideband at  $\omega_0 + \omega_{LO} - \omega_{IF}$ . Similar to the SSB modulation, no other beating signals would contribute to the interested frequency band, thus the proposed scheme is free from the power fading effect.

For multi-band transmission in an OCS system, IBIs will be generated due to the beating between the signals at different frequency bands. For the proposed system, assume that two IF signals at two frequency bands at  $\omega_{IF1}$  and  $\omega_{IF2}$ , the frequency of the light signal will be at  $\omega_0 - \omega_{LO} \pm \omega_{IF1}$  and  $\omega_0 - \omega_{LO} \pm \omega_{IF2}$ . The interband beating signals will be at  $2\omega_{IF1}$ ,  $2\omega_{IF2}$ ,  $\omega_{IF1} + \omega_{IF2}$ ,  $\omega_{IF1} - \omega_{IF2}$ , which are all out of the interested mm-W signal band. Thus, the proposed scheme is free from the IBIs.

### III. EXPERIMENTAL SETUP

The proposed scheme is experimentally evaluated. Fig. 2 shows the experimental setup. A light wave with a wavelength of 1545.62 nm and an optical power of 7 dBm from a LD is sent through PC1 to an MZM. An LO signal with a frequency of 15.75 GHz and a power of 20 dBm generated by a signal generator (Agilent E8254A) is applied to the MZM. By biasing the MZM at the minimum transmission point, two first-order sidebands with a spectral interval of 31.5 GHz are generated. Note that a POF is connected after the MZM to eliminate the residual optical carrier and other high order sidebands. The two first-order sidebands from the POF are then sent to a PM-FBG to generate two orthogonally polarized optical carriers. An EDFA (EDFA1) with a gain of 18 dB is employed to boost the power of the light wave from the MZM before sending it to the PM-FBG. The spectrum of the PM-FBG is shown in Fig. 3. Since the bandwidths of the two transmission bands of the PM-FBG is much larger than the spectral interval between the two optical carriers, instead of filtering out one optical carrier for each polarization state, in the experiment the PM-FBG only filters out one optical carrier for one polarization state (horizontal) and keeping the two optical carriers unchanged for the other polarization state

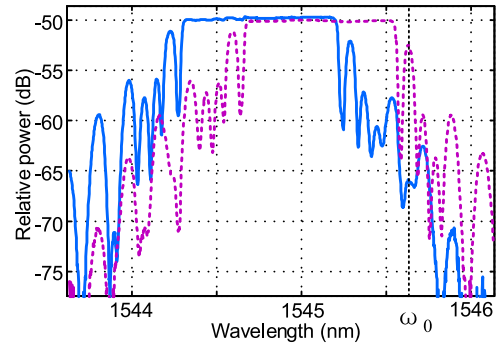


Fig. 3. The optical spectra of the PM-FBG in reflection along the two principal axes.

(vertical), as shown in Fig. 2 at point B. Note that this operation will not change the performance of the proposed signal generation scheme, and the immunity to chromatic-dispersion-induced power fading and IBIs will be still maintained. Then, the light waves are fed to a Sagnac loop via a PBS with the single optical carrier that is horizontally polarized traveling along the counter-clockwise direction, which is modulated by an IF 16-QAM signal at the PolM. The IF 16-QAM signal is generated by an AWG (Tektronix AWG7102) with the IF at 750 MHz. The two optical carriers that are vertically polarized along the clockwise direction pass through the PolM without modulation. The optical signals at the output of the Sagnac loop are combined at the PBS and sent to a second EDFA (EDFA2). After transmission over a 25-km SMF, the orthogonally polarized signals are projected to a Pol, and then photo-detected by a PD (45 GHz, New Focus 1014). The beating between the 16-QAM modulated signal and the unmodulated carriers will generate two mm-W 16-QAM signals at 30.75 and 32.25 GHz. In the experiment, the mm-W signal at 30.75 GHz is used to analyze the performance of the system. Then, the mm-W 16-QAM signals are amplified by a 23 dB electrical amplifier (Agilent 83050A), and sent to a vector signal analyzer (VSA) to evaluate the signal transmission performance. Note that the VSA is implemented using a high-performance real-time oscilloscope (Agilent DSOX93204A) and its associated software package (Agilent 89600A).

### IV. EXPERIMENTAL RESULTS

The performance of the proposed system for the generation and transmission of an mm-W 16-QAM signal with a symbol rate of 500 MSym/s is first evaluated. The IF 16-QAM signal is generated by the AWG, which has an error vector magnitude (EVM) of 3.24%. In the experiment, the optical power at the input of the PD is controlled to be 0 dBm. The spectrum of the generated mm-W 16-QAM signals at 30.75 and 32.25 GHz is shown in Fig. 4(a). The constellation for the signal at 30.75 GHz is shown in Fig. 4(b). Fig. 4(c) and (d) shows the eye diagrams of the signal at 30.75 GHz for the in-phase and quadrature components, respectively. The eye opening can be easily seen. To quantitatively evaluate the errors, the EVM of the signal at 30.75 GHz is calculated, which is 9.9%.

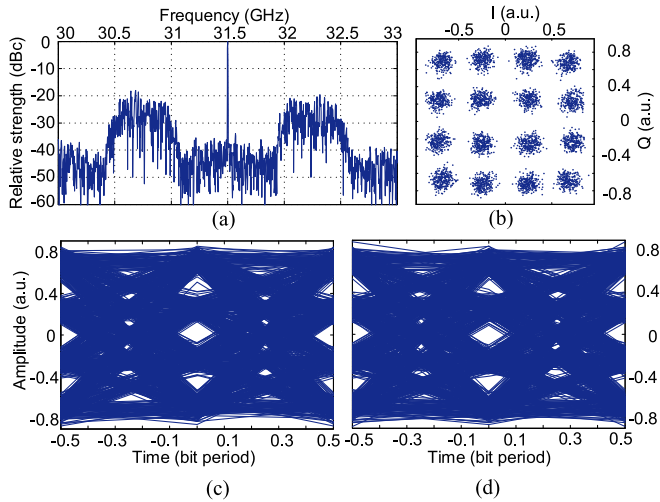


Fig. 4. Experiment results for the generation and transmission of an mm-W signal with a symbol rate of 500 MSym/s. (a) The spectrum of the generated mm-W 16-QAM. (b) The constellation of the generated mm-W 16-QAM signal at 30.75 GHz. (c) The eye diagrams of the in-phase component and (d) the quadrature component of the generated mm-W 16-QAM signal at 30.75 GHz.

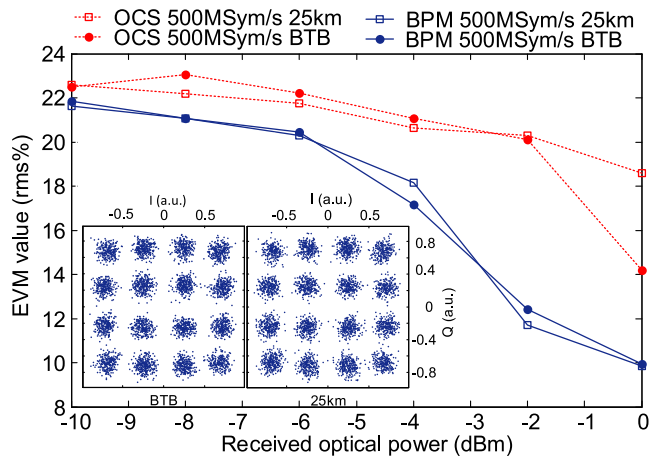


Fig. 5. The EVM measurements as a function of the received optical power for the mm-W signal at 30.75 GHz with a symbol rate of 500 MSym/s for BTB and 25-km transmission (blue-solid lines). The EVM measurements when using OCS modulation are also shown (red-dotted lines).

Then, the EVMs of the generated 30.75 GHz signal as a function of the received optical power for back-to-back (BTB) and 25-km SMF transmission are measured, which are shown in Fig. 5. The constellations for BTB and 25-km transmission with an optical power of 0 dBm at the input of the PD are also shown in Fig. 5. As can be seen no significant deterioration in the constellation is resulted. For comparison, the EVMs when using the OCS modulation are also measured and are shown in Fig. 5. The experimental setup for the OCS modulation is shown in Fig. 6. As can be seen, the use of the proposed scheme has much better performance.

The BER performance is also evaluated, which is done by calculating the EVM through modulation error ratio, which is the measurement of the average SNR for the entire constella-

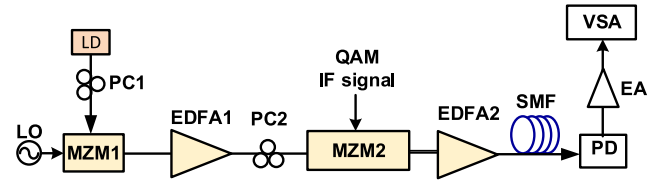


Fig. 6. The experimental setup when using OCS modulation scheme. EA, electrical amplifier; EDFA, erbium-doped fiber amplifier; IF, intermediate frequency; LD, laser diode; LO, local oscillator; MZM, Mach-Zehnder modulator; PC, polarization controller; QAM, quadrature amplitude modulation; PD, photodetector; SMF, single mode fiber.

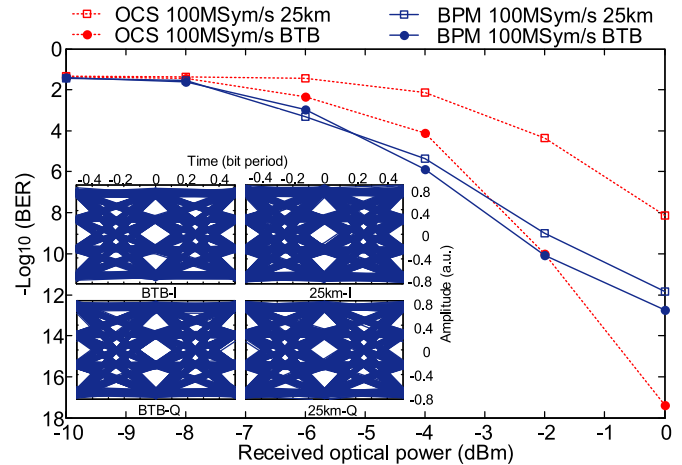


Fig. 7. The BER measurements as a function of the received optical power for the mm-W 16-QAM signal at 30.75 GHz with a symbol rate of 100 MSym/s for BTB and 25-km transmission (blue-solid lines). The BER measurements when using OCS modulation are also shown (red-dotted lines).

tion [20]. In the experiment, the reported results are from raw data without any post-data processing. For the mm-W signal at 30.75 GHz with a symbol rate of 500 MSym/s, the BER after 25-km transmission with the light power at 0 dBm at the input of the PD is  $2.6 \times 10^{-4}$  (or an EVM of 9.84%) which is below the FEC threshold of  $3.8 \times 10^{-3}$  [ $-\log_{10}(\text{BER}) = 2.42$ ]. If the symbol rate is reduced to 100 MSym/s, the BER after 25-km SMF transmission with again the light power at 0 dBm at the input of the PD is as low as  $1.4 \times 10^{-12}$  (or an EVM of 4.8%). The details of the BER measurements are shown in Fig. 7. The eye diagrams for BTB and 25-km transmission with an optical power of 0 dBm at the input of the PD are also shown in Fig. 7. For comparison, the BER measurements when using OCS modulation are also performed and the results are shown in Fig. 7. Again, better performance when using the proposed scheme is achieved.

## V. DISCUSSION AND CONCLUSION

In the experiment, the PD can operate with a maximum input optical power of about 3 dBm. To avoid damaging the PD, we set the input optical power to the PD at 0 dBm, which was the highest received optical power in the experiment. If a PD with a higher maximum input power was used, the performance would be further improved [16].

The proposed technique was demonstrated for downlink signal generation and transmission. In the downlink signal, one optical carrier was not modulated, and it could be reused for uplink transmission. To do so, an optical filter would be needed to select the unmodulated optical carrier. This is an added advantage of the proposed technique to achieve duplex operation with simplified base stations. The clean nature of the reused optical carrier would help improve the uplink transmission performance as compared with those wavelength reuse schemes where the reused optical carrier is not pure and a technique is needed to erase the downlink data [21].

In conclusion, a new approach to generating an mm-W vector signal based on a bi-directional use of a PolM in a Sagnac loop was proposed and experimentally demonstrated. The key advantage of the proposed approach was that the generated mm-W signal was immune to the dispersion-induced power penalty and free from IBBI. In addition, since the modulated and the unmodulated signals are traveling within the same optical path in the Sagnac loop, the phase term of the generated mm-W signal is not affected by the environmental disturbances. Furthermore, the ratio between the powers of the unmodulated and modulated optical carriers can be easily tuned, which would provide a flexible way to optimize the performance of the generated signal. The proposed system was experimentally demonstrated. The generation of a 100 and a 500 MSym/s 16-QAM signals at 31.5 GHz and the transmission of the signals over a 25-km SMF were evaluated. An error-free transmission of the 100 MSym/s signal and the transmission of the 500 MSym/s signal with a BER below the FEC threshold of  $3.8 \times 10^{-3}$  were achieved.

## REFERENCES

- [1] J. Yu, G. K. Chang, Z. Jia, A. Chowdhury, M. F. Huang, H. C. Chien, Y. T. Hsueh, W. Jian, C. Liu, and Z. Dong, "Cost-effective optical millimeter technologies and field demonstrations for very high throughput wireless-over-fiber access systems," *J. Lightw. Technol.*, vol. 28, no. 16, pp. 2376–2397, Aug. 2010.
- [2] J. G. Proakis and M. Salehi, *Digital Communications*, 5th ed. New York, NY, USA: McGraw-Hill, 2007.
- [3] K. Wang, X. Zheng, H. Zhang, and Y. Guo, "A radio-over-fiber downstream link employing carrier-suppressed modulation scheme to regenerate and transmit vector signals," *IEEE Photon. Technol. Lett.*, vol. 19, no. 18, pp. 1365–1367, Sep. 2007.
- [4] T. Shao and J. P. Yao, "Millimeter-wave and UWB over a colorless WDM-PON based on polarization multiplexing using a polarization modulator," *J. Lightw. Technol.*, vol. 31, no. 16, pp. 2742–2751, Aug. 2013.
- [5] J. Yu, Z. Jia, T. Wang, and G. K. Chang, "Centralized lightwave radio-over-fiber system with photonic frequency quadrupling for high-frequency millimeter-wave generation," *IEEE Photon. Technol. Lett.*, vol. 19, no. 19, pp. 1499–1501, Oct. 2007.
- [6] J. Yu, Z. Jia, L. Yi, Y. Su, G. K. Chang, and T. Wang, "Optical millimeter-wave generation or up-conversion using external modulators," *IEEE Photon. Technol. Lett.*, vol. 18, no. 1, pp. 265–267, Jan. 2006.
- [7] A. Kaszubowska, P. Anandarajah, and L. P. Barry, "Multifunctional operation of a fiber Bragg grating in a WDM/SCM radio over fiber distribution system," *IEEE Photon. Technol. Lett.*, vol. 16, no. 2, pp. 605–607, Feb. 2004.
- [8] C. T. Lin, P. T. Shih, W. J. Jiang, E. Z. Wong, J. Chen, and S. Chi, "Photonic vector signal generation at microwave/millimeter-wave bands employing an optical frequency quadrupling scheme," *Opt. Lett.*, vol. 34, no. 14, pp. 2171–2173, Jul. 2009.
- [9] S. H. Fan, C. Liu, and G. K. Chang, "Heterodyne optical carrier suppression for millimeter-wave-over-fiber systems," *J. Lightw. Technol.*, vol. 31, no. 19, pp. 3210–3216, Oct. 2013.
- [10] Y. Zhang, K. Xu, R. Zhu, J. Li, J. Wu, X. Hong, and J. Lin, "Photonic DPASK/QAM signal generation at microwave/millimeter-wave band based on an electro-optic phase modulator," *Opt. Lett.*, vol. 33, no. 20, pp. 2332–2334, Oct. 2008.
- [11] W. J. Jiang, C. T. Lin, C. H. Ho, C. C. Wei, P. T. Shih, J. Chen, and S. Chi, "Photonic vector signal generation employing a novel optical direct-detection in-phase/quadrature-phase upconversion," *Opt. Lett.*, vol. 35, no. 23, pp. 4069–4071, Nov. 2010.
- [12] P. Candelas, J. M. Fuster, J. Martí, and J. C. Roig, "Optically generated electrical-modulation formats in digital-microwave link applications," *J. Lightw. Technol.*, vol. 21, no. 2, pp. 496–499, Feb. 2003.
- [13] R. Sambaraju, V. Polo, J. L. Corral, and J. Martí, "Ten gigabits per second 16-level quadrature amplitude modulated millimeter-wave carrier generation using dual-drive Mach-Zehnder modulators incorporated photonic-vector modulator," *Opt. Lett.*, vol. 33, no. 16, pp. 1833–1835, Aug. 2008.
- [14] J. L. Corral, R. Sambaraju, M. A. Piqueras, and V. Polo, "Generation of pure electrical quadrature amplitude modulation with photonic vector modulator," *Opt. Lett.*, vol. 33, no. 12, pp. 1294–1296, Jun. 2008.
- [15] W. Li and J. P. Yao, "Dynamic range improvement of a microwave photonic link based on bi-directional use of a polarization modulator in a Sagnac loop," *Opt. Exp.*, vol. 21, no. 13, pp. 15692–15697, Jun. 2013.
- [16] G. P. Agrawal, *Fiber-Optic Communication Systems*, 4th ed. Hoboken, NJ, USA: Wiley, 2010.
- [17] M. Li, Z. Li, and J. P. Yao, "Photonic generation of precisely phase-shifted binary phase-coded microwave signal," *IEEE Photon. Technol. Lett.*, vol. 24, no. 22, pp. 2001–2004, Nov. 2012.
- [18] W. Liu, T. Shao, and J. P. Yao, "Ultra-wideband and 60-GHz generation and transmission over a wavelength division multiplexing-passive optical network," *J. Opt. Commun. Netw.*, vol. 5, no. 9, pp. 1076–1082, Sep. 2013.
- [19] W. Liu, M. Wang, and J. P. Yao, "Tunable microwave and sub-terahertz generation based on frequency quadrupling using a single polarization modulator," *J. Lightw. Technol.*, vol. 31, no. 10, pp. 1636–1644, May 2013.
- [20] V. J. Urlick, J. X. Qiu, and F. Bucholtz, "Wide-band QAM-over-fiber using phase modulation and interferometric demodulation," *IEEE Photon. Technol. Lett.*, vol. 16, no. 10, pp. 2374–2376, Oct. 2004.
- [21] G. K. Chang, A. Chowdhury, Z. Jia, H. C. Chien, M. F. Huang, J. Yu, and G. Ellinas, "Key technologies of WDM-PON for future converged optical broadband access networks," *J. Opt. Commun. Netw.*, vol. 1, no. 4, pp. C35–C50, Sep. 2009.

**Ruoming Li** (S'13) received the B.Eng. degree in information engineering from the Changchun University of Science and Technology, Changchun, China, in 2004, and the M.S. degree in optical engineering from Jinan University, Guangzhou, China, in 2007. He is currently working toward the Ph.D. degree as a joint training student in the College of Engineering and Applied Sciences, Nanjing University, Nanjing, China, and the School of Electrical Engineering and Computer Science, University of Ottawa, Ottawa, ON, Canada.

His current research interests include photonic generation of microwave and millimeter-wave signals and radio over fiber.

**Wangzhe Li** (S'08) received the B.E. degree in electronic science and technology from Xi'an Jiaotong University, Xi'an, China, in 2004, the M.Sc. degree in optoelectronics and electronic science from Tsinghua University, Beijing, China, in 2007, and the Ph.D. degree in electrical engineering from the University of Ottawa, Ottawa, ON, Canada, in 2013.

He is currently a Postdoctoral Fellow at the Microwave Photonics Research Laboratory, School of Electrical Engineering and Computer Science, University of Ottawa. His current research interests include photonic generation of microwave and Terahertz signals, arbitrary waveform generation, optoelectronic oscillation, and silicon photonics.

Dr. Li received the 2011 IEEE Microwave Theory and Techniques Society Graduate Fellowship and the 2011 IEEE Photonics Society Graduate Fellowship.

**Xiangfei Chen** (M'05–SM'12) received the Ph.D. degree in physics from Nanjing University, Nanjing, China, in 1996. From 1996 to 2000, he was a Faculty Member with the Nanjing University of Post and Telecommunication Technology, where he was involved in the research and development of fiber optic components. From 2000 to 2006, he was an Associate Professor with the Department of Electrical Engineering, Tsinghua University, Beijing, China, where he was involved in the research and development of novel fiber Bragg grating-based devices and their applications in fiber optic system. From October 2004 to April 2005, he was a Visiting Scholar with the Microwave Photonics Research Laboratory, School of Information Technology and Engineering, University of Ottawa, Ottawa, ON, Canada. He is currently a Professor with the Microwave Photonics Technology Laboratory, the National Laboratory of Solid State Microstructures and the College of Engineering and Applied Sciences, Nanjing University, Nanjing, China. He has authored or coauthored more than 120 journal and conference papers. He also holds a number of patents. His current research interests include the development of photonic integration circuits, novel fiber optic devices for high-speed large-capacity optical networks, microwave photonics, and fiber optic sensors.

**Jianping Yao** (M'99–SM'01–F'12) received the Ph.D. degree in electrical engineering from the Université de Toulon, Toulon, France, in December 1997.

He joined the School of Electrical and Electronic Engineering, Nanyang Technological University, Singapore, as an Assistant Professor in 1998. In December 2001, he joined the School of Electrical Engineering and Computer Science, University of Ottawa, Ottawa, ON, Canada, as an Assistant Professor, where he became an Associate Professor in 2003, and a Full Professor in 2006. He was appointed as the University Research Chair in Microwave Photonics in 2007. From July 2007 to June 2010, he was the Director of the Ottawa-Carleton Institute for Electrical and Computer Engineering. He was reappointed as the Director of the Ottawa-Carleton Institute for Electrical and Computer Engineering in 2013. He is currently a Professor and the University Research Chair in the School of Electrical Engineering and Computer Science, University of Ottawa. He has published more than 460 papers, including more than 260 papers in peer-reviewed journals and 200 papers in conference proceedings.

Dr. Yao was a Guest Editor for the “Focus Issue on Microwave Photonics” in *Optics Express* in 2013 and a “Feature Issue on Microwave Photonics” in *Photonics Research* in 2014. He is currently a Topical Editor for *Optics Letters*, and serves on the Editorial Board of the IEEE TRANSACTIONS ON MICROWAVE THEORY AND TECHNIQUES, *Optics Communications*, and *China Science Bulletin*. He is the Chair of numerous international conferences, symposia, and workshops, including the Vice-Technical Program Committee (TPC) Chair of the IEEE Microwave Photonics Conference in 2007, the TPC Cochair of the Asia-Pacific Microwave Photonics Conference in 2009 and 2010, the TPC Chair of the high-speed and broadband wireless technologies subcommittee of the IEEE Radio Wireless Symposium in 2009–2012, the TPC Chair of the microwave photonics subcommittee of the IEEE Photonics Society Annual Meeting in 2009, the TPC Chair of the IEEE Microwave Photonics Conference in 2010, the General Cochair of the IEEE Microwave Photonics Conference in 2011, the TPC Cochair of the IEEE Microwave Photonics Conference in 2014, and the General Cochair of the IEEE Microwave Photonics Conference in 2015. He received the 2005 International Creative Research Award at the University of Ottawa, and the 2007 George S. Glinski Award for Excellence in Research. He was selected to receive an Inaugural OSA Outstanding Reviewer Award in 2012. He is an IEEE MTT-S distinguished microwave Lecturer for 2013–2015. He is a registered Professional Engineer of Ontario. He is a Fellow of the Optical Society of America and the Canadian Academy of Engineering.